UNIVERSITÀ DEGLI STUDI DI TORINO

A comparative study of the activity of TiO₂ Wackherr and Degussa P25 in the photocatalytic degradation of picloram

Biljana Abramović[1*], Daniela Šojić[1], Vesna Despotović[1], Davide Vione[2], Marco Pazzi[2], János Csanádi[1]

[1]*Department of Chemistry, Biochemistry and Environmental Protection, Faculty of Sciences, University of Novi Sad, Trg D. Obradovića 3, 21000 Novi Sad, Serbia*

[2]*Dipartimento di Chimica Analitica, Università di Torino, Via Pietro Giuria 5, 10125 Torino, Italy*

This paper is dedicated to Vesna Anderluh[#]

[#] In memory of Vesna Anderluh, who was one of initiators of the collaboration from which this work has resulted.

*Professor Biljana Abramović

Department of Chemistry, Biochemistry and Environmental Protection

Faculty of Sciences

Phone: +381 21 4852753

Fax: +381 21 454065

e-mail: biljana.abramovic@dh.uns.ac.rs

Trg D. Obradovića 3

21000 Novi Sad

Serbia

E-mail address: daniela.sojic@dh.uns.ac.rs (Daniela Šojić)
vesna.despotovic@dh.uns.ac.rs (Vesna Despotović)
davide.vione@unito.it (Davide Vione)
marco.pazzi@unito.it (Marco Pazzi)
janos.canadi@dh.uns.ac.rs (János Csanádi)

Abstract

A comparative study was carried out of the efficiency of titanium dioxide specimens Wackherr and Degussa P25 toward the photocatalytic degradation of picloram, a widely used herbicide. The study encompassed transformation kinetics and efficiency, identification of intermediates and reaction pathways. In the investigated range of initial concentrations (0.25 – 1.0 mM), the photocatalytic degradation of picloram in the first stage of the reaction followed approximately a pseudo-first order kinetics. The TiO_2 Wackherr induced significantly faster picloram degradation than TiO_2 Degussa P25 when high photocatalyst loadings and high substrate concentrations were used. By examining the effect of ethanol as a hydroxyl radical scavenger, it was shown that the photocatalytic degradation of picloram takes place mainly via the hydroxyl radicals, while the valence-band holes play a less important role. Total organic carbon analysis showed that complete mineralization of picloram occurred after about 16 hours of irradiation. Several degradation intermediates were identified by using LC–MS, GC–MS, and ^{1}H NMR, which allowed the proposal of a tentative pathway for the photocatalytic transformation of picloram. Finally, the photocatalytic degradation rates of three selected herbicides (picloram, triclopyr and mecoprop) were compared, and the results show that the efficiency of photocatalytic degradation is greatly influenced by the molecular structure.

Keywords: Picloram; Herbicide; Photocatalysis; Titanium dioxide; Photocatalytic degradation pathways

1. Introduction

Over the last few decades, water pollution has become an issue of worldwide concern. For this reason, intense research attention has been paid to the removal of pollutant loads from wastewater effluents [1]. Hazardous contaminants such as pesticides constitute a serious risk for human health due to their high toxicity. The widespread use of pesticides can result in contamination of surface and ground waters in the areas of their application [2]. Furthermore, bioaccumulation and biomagnification can lead to hazardous concentrations in humans. Among the chemicals that are likely to be found in groundwater, pesticides have a non-negligible presence and their elimination is necessary, especially if the water is intended for human consumption. Recent progress in water treatment has led to the development of advanced oxidation processes (AOPs) [3].

Pyridine and pyridine derivatives have received wide attention because of their occurrence in the environment and their hazardous effects on ecosystems and human health [4]. Picloram (4-amino-3,5,6-trichloro-2-pyridincarboxylic acid) is a potent herbicide that effectively controls the growth of broadleaf weed in pasture and rangeland, as well as in fields cultivated for wheat, barley, oats and woody plant species [5]. However, picloram residues were detected to a soil depth of 2.4 m, after 1 year following the application of 1.12 kg/ha picloram [6]. Indeed, picloram is moderately to highly persistent in the soil environment, with reported field half-lives ranging from 20 to 300 days and an estimated average of 90 days [7]. Degradation by microorganisms is mainly aerobic and depends on the application rate. Picloram is poorly bound to soil and its water solubility (440 mg/L) makes it a potentially mobile compound [8]. These properties, combined with persistence, mean that the use of picloram can cause groundwater contamination. As reported in the literature, it is one of the pesticides that is most often found in drinking water [9]. The degradation and removal of picloram was investigated by several authors. Ghauch [10] used zero-valent iron (ZVI) for degrading picloram, which was converted into 4-amino-2-pyridylcarbinol in 1 hour. However, picloram degradation to non-hazardous species was not complete. Heterogeneous photocatalysis in the presence of different kinds of TiO_2 catalysts [11] and the electro-Fenton process [12] were also investigated.

Adsorption processes using calcinated hydrotalcite [13] and calcinated Mg–Al–CO₃–LDH [14] as sorbents have also been adopted for the removal of picloram from water [15], but these physical treatments do not solve the problem of contaminant degradation after adsorption.

The goal of this work was to make a detailed comparison of the efficiency, kinetics and mechanism of photodegradation of picloram in the presence of two TiO_2 specimens that differ for particle size, radiation absorption and scattering properties, namely TiO_2 Wackherr and Degussa P25. The study was carried out under a variety of experimental conditions; the effects of initial concentration of picloram, catalyst loading and presence of an hydroxyl radical scavenger were studied. An attempt has also been made to identify the reaction intermediates formed during the photo-oxidation process, using LC–MS, GC–MS and ^{1}H NMR techniques. Finally, with the aim of investigating the link between catalyst activity and molecular structure, the photocatalytic activity of triclopyr and mecoprop (Fig. 1) was also studied, because of their wide use for selective control of many annual and some perennial weeds, and because of their occurrence in drinking water [9,16].
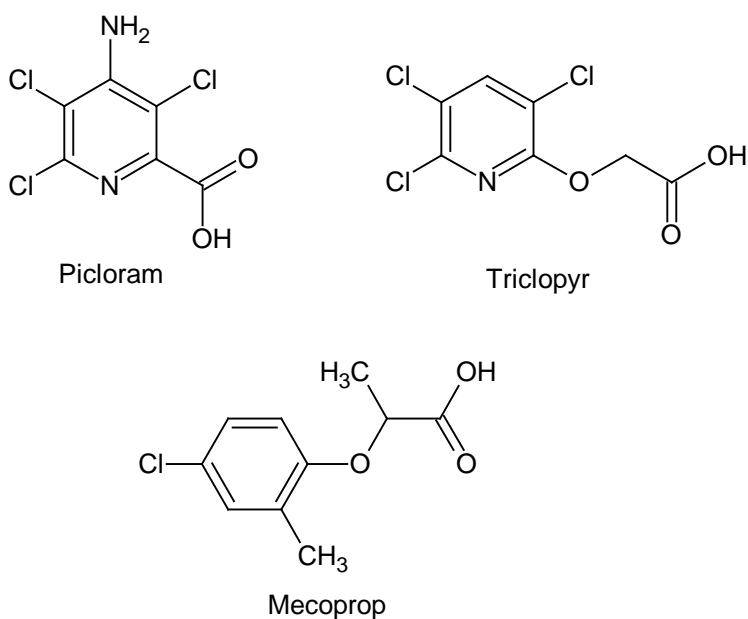

Fig. 1. Structures of the studied herbicides.

2. Materials and methods

2.1. Chemicals and solutions

All chemicals were of reagent grade and were used without further purification. Picloram, 99.4% and triclopyr, 99.8%, pestanal quality, were both purchased from Riedel-de Haën.. The commercial herbicide mecoprop (98% purity), obtained from the Chemical Factory "Župa" Kruševac, Serbia, was purified by conventional recrystallization from water–ethanol (1:1, v/v) solution. The purity of purified mecoprop was confirmed by ^{1}H NMR spectrometry (Bruker AC-250). The other chemicals used in this study, such as 35% HCl and 85% H_3PO_4 were purchased from Lachema, Neratovice; 96% ethanol was obtained from Centrohem, Stara Pazova; 98.0% formic acid and 99.9% dichloromethane were obtained from Merck, while 99.8% acetonitrile (ACN) was a product of J. T. Baker. In all experiments doubly-distilled water was used, except for the ^{1}H NMR measurements where D_2O (Aldrich, 99.9% purity) was applied as solvent. Wackherr's "Oxyde de titane standard" (anatase form, surface area 8.5 ± 1.0 m^2/g, crystallite size 300 nm [17], hereafter "TiO$_2$ Wackherr"), produced by the sulfate process and TiO$_2$ Degussa P25 (75% anatase and 25% rutile form, surface area 50 ± 15 m^2/g, crystallite size about 20 nm, non-porous [17]) were used as photocatalysts.

2.2. Photodegradation Procedures

Photocatalytic degradation was carried out in a cell made of Pyrex glass (total volume of *ca.* 40 mL, liquid layer thickness 35 mm), with a plain window on which the light beam was focused. The cell was equipped with a magnetic stirring bar and a water circulating jacket. A 125 W high-pressure mercury lamp (Philips, HPL-N, emission bands in the UV region at 304, 314, 335 and 366 nm, with maximum emission at 366 nm), together with an appropriate concave mirror, was used as the radiation source. Irradiation in the visible spectral range was performed using a 50 W halogen lamp (Philips) and a 400 nm cut-off filter. The outputs for the mercury and halogen lamps

were calculated to be ca. 8.8×10^{-9} Einstein/(mL min) and 1.7×10^{-9} Einstein/(mL min) (potassium ferrioxalate actinometry), respectively.

In a typical experiment and unless otherwise stated, the initial picloram, triclopyr and mecoprop concentrations were 1.0 mM and the TiO_2 loading (Wackherr or Degussa P25) was 2.0 mg/mL. The total suspension volume was 20 mL. The aqueous suspension of TiO_2 was sonicated (50 Hz) in the dark for 15 min before illumination, to uniformly disperse the photocatalyst particles and attain adsorption equilibrium. The suspension thus obtained was thermostated at 25 ± 0.5 ℃ (except for the case when the influence of temperature was investigated) in a stream of O_2 (0.5 mL/min), and then irradiated. During irradiation, the mixture was stirred at a constant rate under continuous O_2 flow. Control experiments carried out under O_2 flow but by stopping the irradiation showed that there were no losses of volatile compounds during the degradation. All experiments were performed at the natural pH. Where applicable, ethanol (400 μL) was added as a hydroxyl radical scavenger. Irradiation was then carried out by the standard procedure already described.

2.3. Analytical Procedures

For the LC–DAD studies of photodegradation, aliquots of 0.50 mL were taken from the reaction mixture at the beginning of the experiment and at regular time intervals. Aliquot sampling caused a maximum volume variation of *ca.* 10% in the reaction mixture. Each aliquot was added with 5.0 mL of 0.1 M HCl, and the system was diluted to 10.00 mL with doubly distilled water. The rationale for the addition of HCl is referred to the need of carrying out HPLC and spectrophotometric measures on the same samples. Acidification is required to obtain suitable absorption spectra of picloram. The suspensions containing the photocatalyst were filtered through Millipore (Millex-GV, 0.22 μm) membrane filters. Lack of adsorption of picloram on the filters was preliminary checked. After that, a 20-μl sample was injected and analyzed on an Agilent Technologies 1100 Series liquid chromatograph, equipped with an Eclypse XDB-C18 column (150 mm × 4.6 mm i.d., particle size 5 μm, 25 °C). The UV/VIS DAD detector was set at the absorption maxima (224 nm for picloram, 230 nm for triclopyr and 228 nm for mecoprop). The mobile phase (flow rate 1 cm^3/min) was a

mixture of acetonitrile and water (3:7, v/v, pH 2.56 for picloram, 4:6, v/v, pH 2.62 for triclopyr and 1:1, v/v, pH 2.68 for mecoprop), the water being acidified with phosphoric acid. Reproducibility of repeated runs was around 5-10%.

Absorption spectra were recorded on a double-beam T80+ UV–Vis Spectrophotometer (UK) at a fixed slit width (2 nm), using 1 cm quartz cells and computer-loaded UV Win 5 data software. Kinetics of the pyridine ring degradation was monitored at 224 nm (picloram) [18] and 230 nm (triclopyr). In the case of mecoprop, the aromatic ring degradation was monitored at 228 nm.

For ion chromatographic determinations, aliquots of 0.50 mL of the reaction mixture were taken at regular time intervals and diluted to 10.00 mL. The obtained suspensions were filtered through membrane filters and analyzed on an ion chromatograph Dionex ICS 3000. For anion determination, use was made of an Ion Pac AS18 Analytical column (250 mm × 4 mm) and a conductometric detector. The mobile phase was a solution of KOH (20–40 mM), flow rate 1 mL/min. Cations were determined using an Ion Pac CS12A Analytical column (250 mm × 4 mm) and a conductometric detector. The mobile phase was a solution of 40 mM methane sulfonic acid at a flow rate of 1 mL/min.

In all the cases, correlation coefficients obtained for the calibration curves were higher than 0.99. Changes in the pH during the degradation were monitored using a combined glass electrode (pH-Electrode SenTix 20, WTW) connected to a pH-meter (pH/Cond 340i, WTW).

For the LC–MS evaluation of intermediates, a more concentrated solution (1.5 mM) of picloram was prepared. Aliquots were taken at the beginning of the experiment and at regular time intervals during irradiation. Filtration was carried out to separate the TiO_2 particles without subsequent dilution. Then, a 10 µl sample was injected and analyzed on an Agilent Technologies 1200 series LC with Agilent Technologies 6410 series electrospray ionization triple-quadrupole MS/MS, using Agilent Technologies Zorbax SB-C18 column (30 mm × 2.1 mm i.d., particle size 3.5 µm, 25 °C). The mobile phase (flow rate 0.5 mL/min) consisted of 1 % aqueous formic acid and ACN (gradient: 0 min 10% ACN, 2 min 90% ACN, 6 min 90% ACN, post time 3 min). Analytes were ionized using the electrospray ion source, with nitrogen as drying gas (temperature 350 °C, flow 9 L/min) and nebulizer gas (35 psi),

and a capillary voltage of 4.0 kV. High-purity nitrogen was used as the collision gas. Full scan mode (m/z range 100−600, scan time 250 ms, fragmentor voltage 80 V), using both polarities, was adopted to examine isotopic peaks distribution and obtain structural information.

For the GC–MS characterization of the intermediates, aqueous solutions of 1.5 mM picloram were prepared. After irradiation, the photocatalyst was removed by filtration. The filtrate was extracted with dichloromethane and evaporated to dryness. Each sample was reconstructed with 1 mL dichloromethane. The resulting solution was shaken at room temperature for 5 min, an aliquot was transferred into a vial and injected into a capillary gas chromatograph (Agilent 6890) coupled with a mass spectrometer (Agilent 5973 inert). The injection system used was a Gerstel CIS4 PTV. Initial injection temperature was 50 °C, programmed at 10 °C/s; final temperature was 300 °C, held for 10 min. The injection volume was 2 µl in the splitless mode. The capillary column used was a HP-5MS, 30 m × 0.25 mm × 0.25 µm film thickness. Initial column temperature was 50 °C and was increased by 15 °C/min to 320 °C. The carrier gas was ultrapure He (1.0 mL/min; SIAD, Bergamo, Italy). The ionization source worked in the electronic impact (EI) mode and the mass spectrometer worked in the Scan mode. Identification of spectra was performed using the Wiley 7n library (Agilent Part No. G1035B).

The ^{1}H NMR spectral profiles of picloram/D_2O solutions (1.5 mM, sample volume 1.0 mL) during illumination in the presence of TiO_2 particles were monitored on a Bruker AC-250 instrument.

For total organic carbon (TOC) analysis, samples were irradiated at different time intervals and analyzed after filtration on an Elementar Liqui TOC II analyzer.

3. Results and discussion

3.1. Effects of the kind of TiO_2 and type of irradiation

The photocatalytic activity of TiO_2 Wackherr was compared to that of the most often used Degussa P25 under UV and visible irradiation (Fig. 2). As can be seen from the figure, practically no degradation was observed in the presence of visible light, either

with or without TiO_2. The lack of picloram disappearance with TiO_2 under these conditions also allows the exclusion of a significant adsorption of picloram on the catalyst surface during the course of the irradiation. In contrast, significant picloram degradation could be observed under UV, and the process involving TiO_2 Wackherr was significantly faster compared to Degussa P25. However, TiO_2 Wackherr yielded more intermediates and at relatively higher concentration (Fig. 3a) than Degussa P25 (Fig. 3b).
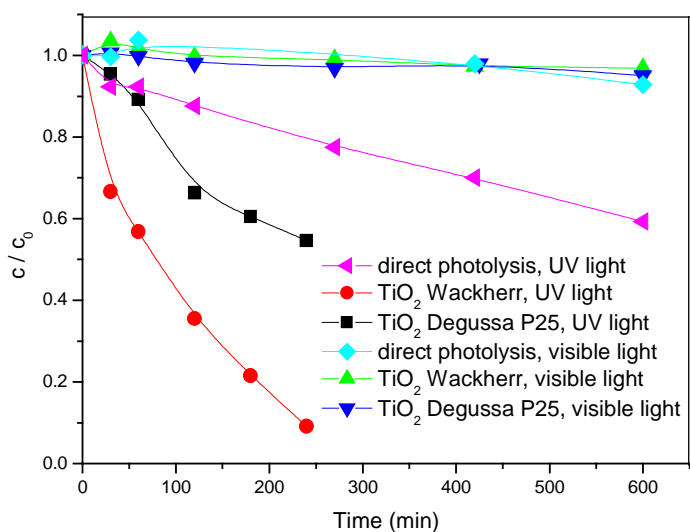

Fig. 2. Kinetics of the photolytic and photocatalytic degradation of picloram ($c_0 = 1.0$ mM). When present, the TiO_2 loading was 2.0 mg/mL.
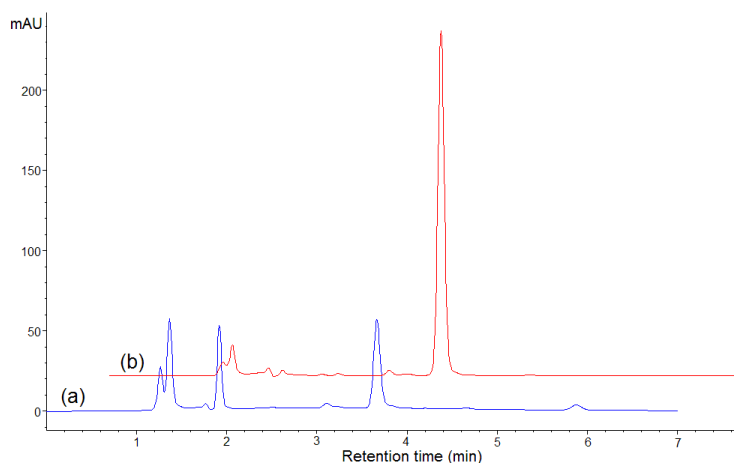

Fig. 3. Chromatograms obtained after 120 min of picloram degradation under UV irradiation in the presence of TiO_2 Wackherr (a) and TiO_2 Degussa P25 (b). $\lambda_{det} = 224$ nm, RT(picloram) = 3.7 min.

The faster degradation of picloram in the presence of TiO_2 Wackherr is noteworthy, considering that this TiO_2 specimen has much larger particles (average radii in solution are 3-4 times larger [17]) than Degussa P25 and a surface area that is almost six times lower [17].

The direct photolysis of picloram was also checked under the adopted irradiation conditions, in the absence of catalysts (Fig. 2). It is shown that picloram can be degraded by direct photolysis in the near-UV region, but at a significantly lower rate compared to the photocatalytic process, especially in the case of TiO_2 Wackherr. It should also be considered that radiation absorption and scattering by TiO_2 can substantially inhibit the direct photolysis processes under photocatalytic conditions [19]. From the extinction spectra of TiO_2 Wackherr and Degussa P25 [17], it can be derived that at 366 nm (the wavelength of maximum emission of the adopted lamp) both TiO_2 specimens at 2.0 mg/mL loading would be able to filter out the near totality of the incident radiation (extinction E > 10). Under such conditions, the rate of the direct photolysis is expected to be negligible. An even more extreme scenario would be operational at $\lambda < 366$ nm.

3.2. Effect of operational parameters on the photocatalytic degradation of picloram

AOPs rely on the generation and subsequent reaction of highly reactive transient species (often the $^\bullet OH$ radical), and there are many factors that can affect the efficiency of the process. The present study encompassed the effect of initial picloram concentration, amount of catalyst, and presence of hydroxyl radical scavengers.

3.2.1. Effect of the initial concentration of picloram

The effect of the initial concentration of picloram on the rate of its photodegradation was investigated in the range of concentrations from 0.25 to 1.0 mM. Under the relevant experimental conditions the reaction followed a pseudo-first order kinetics (the linear correlation coefficients were in the range of 0.980–0.999). On the basis of the kinetic curves ln *c* (substrate concentration) vs. *t* (irradiation time up to 120 min),

the values of the pseudo-first order rate constant k' were calculated for all the investigated initial concentrations of picloram (c_0). The initial rates of picloram transformation were calculated as the product $k' \cdot c_0$. They are reported in Fig. 4 as a function of c_0.

Note the faster transformation rates by TiO_2 Wackherr compared to Degussa P25. This is a very interesting finding because earlier studies have shown that TiO_2 Degussa P25 showed a higher photocatalytic activity than most other readily available (commercial) TiO_2 specimens [20] (by the way, TiO_2 Wackherr is also commercially available).

Fig. 4 also shows that for both photocatalysts the trend of the photodegradation rate is not proportional to the increase of picloram concentration. This is often found in photocatalysis [21,22]. In particular, the decrease of the degradation rate above a certain substrate concentration is thought to be due to the combination of direct and reverse (back) reactions [23].
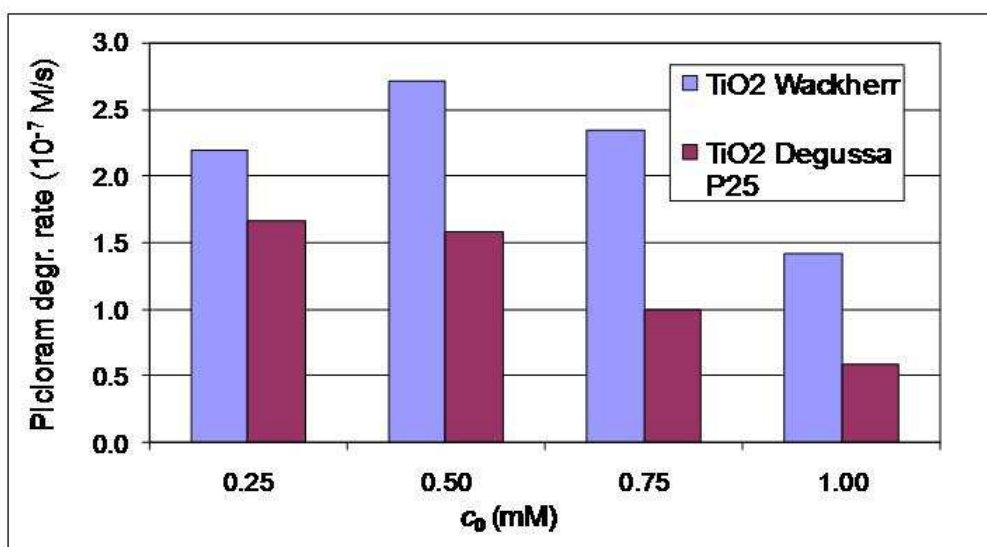

Fig. 4. Effect of the initial concentration of picloram (c_0) on the initial rate of its decomposition, in the presence of TiO_2 Wackherr and Degussa P25. In both cases the TiO_2 loading was 2.0 mg/mL.

Because most organic compounds require a two-electron oxidation to yield the transformation intermediates, after abstraction of one electron or addition of $^\bullet OH$ one gets radical species that may be adsorbed to the catalyst surface. In competition with

further oxidation, the organic transients can be reduced back to the initial substrate by valence-band electrons. The back reactions are detrimental to photocatalytic degradation. They depend on both the substrate and the photocatalyst, and their importance increases with increasing substrate concentration [23].

Fig. 4 shows a decrease of picloram degradation rate above 0.25 mM initial picloram for Degussa P25, and above 0.50 mM for TiO_2 Wackherr. These trends imply that the back reactions of picloram are more important in the case of TiO_2 Degussa P25. By comparing the rather similar degradation rates of picloram with the two photocatalysts at $c_0 = 0.25$ mM, and the considerable difference at $c_0 = 1.00$ mM, it can be inferred that the less important role of the back reactions is a key factor to account for the considerably higher photocatalytic activity of TiO_2 Wackherr at the highest studied substrate concentration.

An alternative explanation for the effect of the substrate concentration is the competition for reactive species between the substrate and the transformation intermediates, the concentration of which would increase with increasing substrate, or the poisoning of the photocatalyst surface by the intermediates themselves. However, late intermediates could not have an important impact on the initial degradation rates. Moreover, TiO_2 Wackherr was shown to produce more intermediates and at a higher concentration than P25 (see Fig. 3), thus one would expect a more important decrease of the degradation rate with substrate concentration for the Wackherr photocatalyst, which is clearly not the case.

3.2.2. Effect of catalyst loading

The effect of the loading of TiO_2 Wackherr and of Degussa P25 on the efficiency of picloram photodegradation was examined in the loading range from 0.25 to 2.0 mg/mL (Fig. 5).

As can be seen in Fig. 5, the effect of catalyst loading on the photocatalytic degradation of picloram is strongly influenced by the kind of TiO_2 used. In the case of TiO_2 Wackherr, the degradation efficiency steadily increased with the loading. As far as TiO_2 Degussa P25 is concerned, one gets a trend with a plateau above 0.5 mg/mL photocatalyst. These results are in agreement with literature data of phenol and benzoic

acid degradation, and suggest that the different behavior of the two photocatalysts could be a consequence of the difference in the optical properties [17].
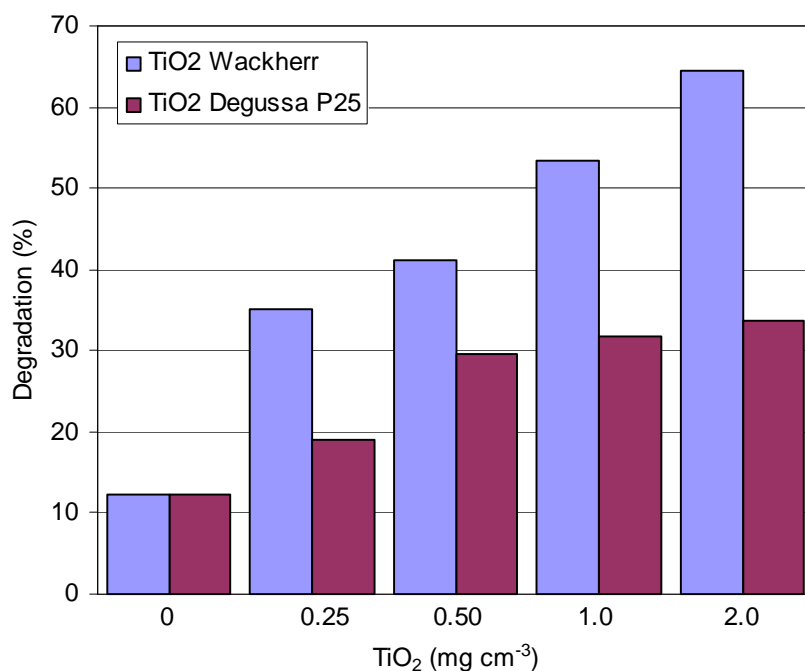

Fig. 5. Influence of the catalyst loading on the efficiency (%) of picloram degradation after 120 min of irradiation. Initial picloram concentration was 1.0 mM.

Indeed, TiO_2 Wackherr and Degussa P25 have similar neperian absorption coefficients κ^* ($2.7 \cdot 10^3$ vs. $3.4 \cdot 10^3$ cm^2/g at 360 nm, respectively), but the scattering coefficient σ^* of Degussa P25 is significantly higher ($9.2 \cdot 10^4$ cm^2/g at 360 nm, to be compared with $5.5 \cdot 10^4$ cm^2/g for TiO_2 Wackherr) [17]. This means that TiO_2 Wackherr makes a more efficient use of the incident radiation than Degussa P25, because a higher fraction of radiation is absorbed instead of being scattered. Scattering inhibits the photodegradation processes, and its effect becomes more significant when the photocatalyst loading is higher [23,24]. In the case of TiO_2 Wackherr, the lower scattering would account for the steady increase of degradation efficiency with photocatalyst loading, differently from P25.

3.2.4. Effect of ethanol as hydroxyl radical scavenger

Photocatalytic degradation processes can involve either reaction between the substrate and surface-adsorbed $^{\bullet}$OH groups, or direct charge-transfer processes with valence-band holes [17]. Aromatic compounds are usually reactive with valence-band holes, while addition of alcohols or glycols is a good strategy to selectively block the $^{\bullet}$OH-mediated processes [25,26].

In order to investigate whether the photocatalytic degradation of picloram takes place via $^{\bullet}$OH, ethanol (400 μL, *i.e.* 0.34 M in the final solution) was added to the reaction mixture containing picloram and TiO_2 Wackherr or Degussa P25. The results are presented in Fig. 6 and show that ethanol considerably inhibited the photocatalytic degradation of picloram. The experimental data imply that the photocatalytic degradation of picloram mainly proceeds via $^{\bullet}$OH, especially in the case of TiO_2 Wackherr, while valence-band holes are expected to play a secondary role.

3.3. Evaluation of the degree of mineralization

Since picloram contains three covalently bound chlorine atoms, which could be converted to chloride during the photocatalytic degradation, the transformation reaction can also be monitored by measuring the chloride release in the presence of TiO_2 (Fig. 7a/b, curves #1).
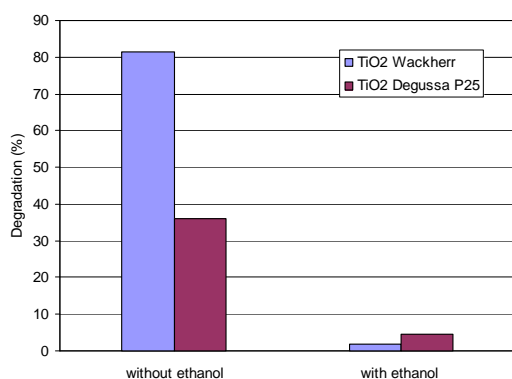

Fig. 6. Effect of 0.34 M ethanol on the efficiency of degradation of picloram in the presence of TiO_2 after 120 min of irradiation.
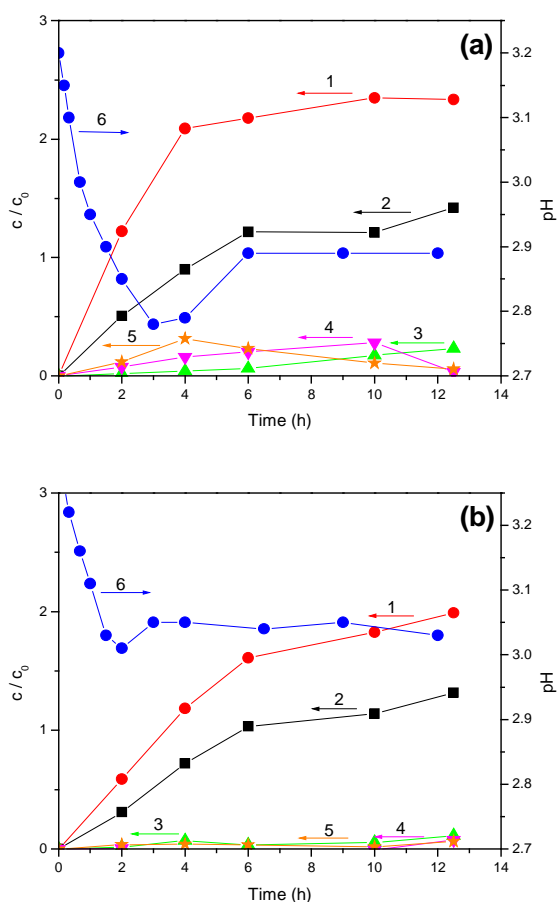
Fig. 7. Photocatalytic degradation of picloram in the presence of TiO$_2$ Wackherr (a) and TiO$_2$ Degussa P25 (b). Evolution of Cl$^-$ (curve 1); NH$_4^+$ (2); NO$_3^-$ (3); acetate ion (4); formate ion (5) and pH (6).

It was found that the reaction rate constant of chloride release in the presence of TiO$_2$ Wackherr or Degussa P25 was approximately two times lower than the rate constant of the 224-nm absorbance decrease (see Fig. 8), the latter being a measure of pyridine ring degradation [18]. The faster degradation of the ring compared to the chloride release suggests the formation of aliphatic intermediates containing Cl.
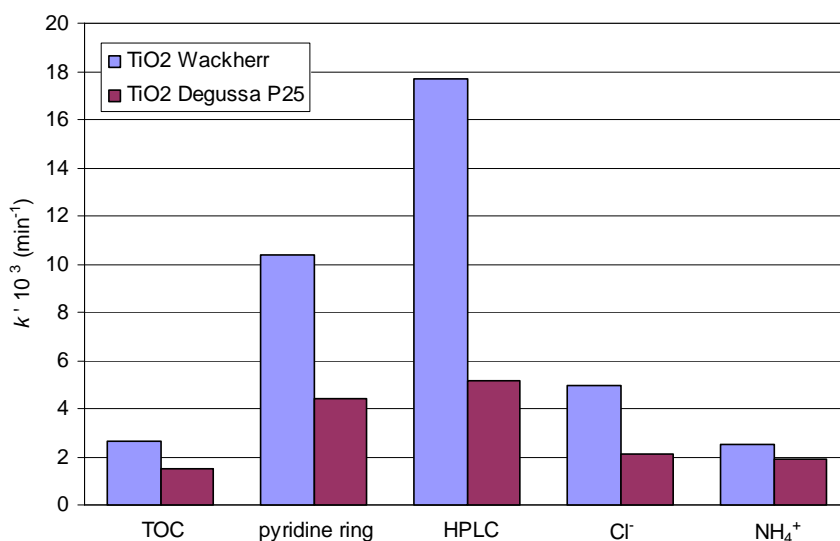
Fig. 8. Comparison of the reaction rate constants for photocatalytic degradation and mineralization of picloram, calculated over 240 min of irradiation.

Moreover, the degradation rate constant obtained from the spectrophotometric kinetic curve (A_{224nm}) was lower than the rate constant of picloram transformation obtained by HPLC (Fig. 8). This finding suggests that the degradation process is accompanied by the formation of intermediates that retain the pyridine ring. The observed difference in the degradation rate constants was especially pronounced when using TiO_2 Wackherr. This indicates that TiO_2 Wackherr induces the formation of a higher amount of intermediates with a pyridine ring compared to Degussa P25, which is in agreement with the chromatograms reported in Fig. 3a/b.

During the photocatalytic degradation, organic nitrogen is mainly transformed into ammonium and/or nitrite/nitrate, and sometimes into N_2 [27]. The ratio of ammonium to nitrate depends on the chemical structure of the substrate and on the reaction conditions [28]. In the present case both ammonium and nitrate were monitored, and the results show that practically only ammonium ions were formed (Fig. 7a/b, curves #2, compared to curves #3 for nitrate).

In the case of both TiO_2 specimens, the rate constant for the formation of ammonium was about two to four times lower compared to the rate constant for pyridine ring degradation (see Fig. 8). Such a finding suggests that the fragmentation of the pyridine ring does not necessarily involve the release of nitrogen, which is

17

compatible with the formation of nitrogen-containing intermediates having an acyclic structure. This is in agreement with previous results obtained in the study of the degradation of 2-amino-5-chloropyridine [29], 3-amino-2-chloropyridine [27], and 3-chloropyridine [30]. Fig. 7 also suggests that, for both TiO_2 specimens, after 12 h irradiation around two thirds of the organic chlorine was released as Cl^- and a comparable fraction of the organic nitrogen was transformed into NH_4^+.

A decrease of pH by 0.2-0.3 units was also observed (Fig. 7, curve #6). It could be due to the release of chloride (as $H^+ Cl^-$) being faster than that of ammonium, the latter consuming H^+ [31] (compare curves #2 –chloride– and #3 –ammonium– in Fig. 7).

Under the adopted experimental conditions one also finds acetate and formate (Fig. 7a/b, curves #4 and #5), which are well known to yield CO_2 and H_2O by photocatalysis [32]. Therefore, one can hypothesize that the final mineralization products of picloram would be CO_2, H_2O, Cl^- and NH_4^+, with a very small amount of NO_3^-. These data are in agreement with previous results obtained with clopyralid, which also belongs to the same class of pyridine derivatives [33]. The TOC measurements showed a complete mineralization of picloram after about 16 hours irradiation, in the presence of both TiO_2 specimens. However, the parent compound degraded significantly faster with TiO_2 Wackherr than with Degussa P25.

3.4. Intermediates and mechanism of photodegradation

The photochemical degradation of pesticides is often accompanied by the formation of intermediates that can potentially be harmful to the environment [34,35]. Several techniques were adopted in this work to study the intermediates of picloram photodegradation: LC–MS, GC–MS and ^{1}H NMR. The same compounds, although in different amounts, were identified with both TiO_2 Wackherr and Degussa P25. However, TiO_2 Wackherr additionally induced the formation of some unidentified molecules (see Fig. 3). The LC–MS technique identified compounds **1** (picloram) and **3** (see Fig. 9) based on their MS/MS fragmentation data, given below (PI: positive ionization; NI: negative ionization; compound numbers are referred to the structures reported in Fig. 9):

Compound 1:

NI: [M–H]⁻ (*m/z* 239, 100%, A+2 96.8%, A+4 33.2%), [M–H–CO₂]⁻ (*m/z* 195, 72.0%, A+2 67.9%, A+4 20.7%),

PI: [M+Na]⁺ (*m/z* 263, 10.6%), [M+H]⁺ (*m/z* 241, 100%, A+2 96.3%, A+4 30.1%), [M+H–H₂O]⁺ (*m/z* 223, 3.78%)

Compound 3:

NI: [M–H]⁻ (*m/z* 221, 100.0%, A+2 63.1%, A+4 10.3%), [M–H–CO₂]⁻ (*m/z* 177, 14.6%, A+2 8.76%),

PI: [M+Na]⁺ (*m/z* 245, 12.3%), [M+H]⁺ (*m/z* 223, 100.0%, A+2 66.4%, A+4 9.92%), [M+H–H₂O]⁺ (*m/z* 205, 18.7%)

By GC-EI-MS it was possible to identify compound **2** by comparison with spectra libraries. The EI spectrum of **2** is summarized below (the *m/z* values separated by a hyphen have been attributed to the isotopic patterns of chlorine):

Compound 2: m/z 230-232-234 (M+), 203-205-207, 195-197, 168-170, 141, 132, 125, 118, 109-111, 97-97, 81-83, 69-71, 57, 56, 44, 43.

Identification of the intermediates was also carried out by ¹H NMR. The proton spectrum recorded for picloram solution in D₂O before irradiation contained no signal that would belong to the starting compound. This is understandable when bearing in mind that there is no proton directly bound to the pyridine ring and that the other protons can be exchanged with D₂O. The only detected signal at about 4.8 ppm would represent the moisture present in D₂O. The ¹H NMR spectral analysis indicated that the largest number of signals appeared after 2-4 h of photocatalytic degradation (at 8.00, 7.65 and 6.15 ppm). This means that the majority of intermediates with D₂O non-exchangeable hydrogen atoms are formed within this time interval. The most pronounced signal at 6.15 ppm was observed after 2 h irradiation, while the intensity of the signal at 8.00 ppm increased up to about 4 h. All the signals in the ¹H NMR spectra disappeared after 9 h. The appearance of the above signals can be explained by the formation of intermediates shown in Fig. 9 (**2**, **3**, **4**). The appearance and the

change of the signal at 8.00 ppm illustrates, most probably, the course of the reaction of reductive desamination that generates the intermediate **4** (Fig. 9).
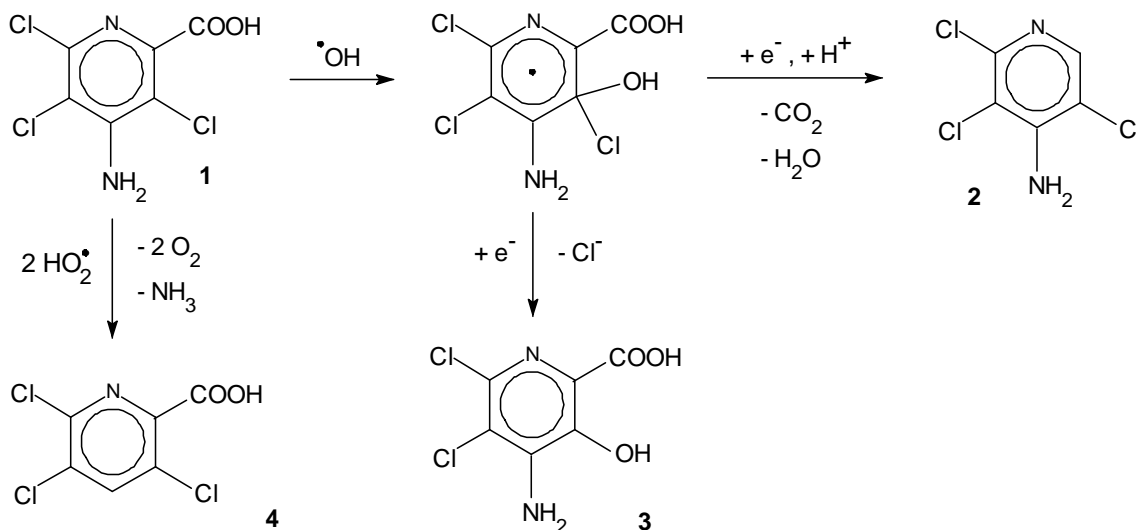

Fig. 9. Tentative pathways for the photocatalytic degradation of picloram (**1**) in the presence of TiO_2 Wackherr and Degussa P25.

Similar intermediates of picloram, **2**, **3** and **4**, were reported by Rahman and Muneer during the photocatalytic degradation on TiO_2 [11]. Özcan et al. additionally identified the 5,6-dichloro-3-hydroxypyridine-2-carboxylic acid in the electro-Fenton process [12]. Ghauch also reported the formation of some intermediates and a final product, the 4-amino-2-pyridylcarbinol, by using ZVI reduction [10]. Understandably, given the reductive conditions of ZVI, the reported intermediates were different from those obtained in our system.

Based on the identified intermediates it is possible to propose a tentative scheme of picloram photocatalytic degradation (Fig. 9). First of all, it should be considered that both the loss of the carboxylic group (**1** → **2**) and the replacement of a chlorine atom with a hydroxyl group (**1** → **3**) require combination of an oxidative and a reductive step. The marked inhibition effect of ethanol, added as •OH scavenger (Fig. 6), suggests that the reductive steps might not be rate-determining. Therefore, it is likely that the primary reaction of picloram is an oxidative step. That could involve •OH, in keeping with the results obtained upon addition of ethanol. The radical •OH could attack picloram by ring addition, forming a radical addition transient that could evolve

into **2** (4-amino-2,3,5-trichloropyridine) by reductive elimination of water and CO_2. In contrast, reductive elimination of chloride from the radical transient could yield **3** (4-amino-2,3-dichloro-5-hydroxy-picolinic acid). The formation of **4** (3,5,6-trichloropyridine-2-carboxylic acid) involves a completely reductive process. Addition of two hydrogen atoms to picloram would reductively break the bond between the amino group and the ring, leading to **4** upon release of ammonia.

To enhance the reliability of identification of the intermediates, the degradation mechanism was studied at a somewhat higher concentration of picloram (1.5 mM) compared to that used to study the effects of operational parameters (1.0 mM). However, this small increase in the picloram concentration could not affect the degradation mechanism significantly. This statement is supported by the nature of the identified intermediates, which do not include dimeric species that are usually observed in the presence of an elevated initial concentration of the substrate.

3.5. Effect of herbicide structure

In order to examine the effect of the substrate structure on the efficiency of photocatalytic degradation, other two herbicides where chosen, *viz.* triclopyr and mecoprop. Their degradation kinetics was studied in the presence of both Wackherr and Degussa P25, under the optimal conditions found for picloram. Triclopyr was selected because it has a pyridine ring like picloram but different substituents, whereas mecoprop has an aromatic ring with somewhat different substituents (see Fig. 1). Figs. 10 and 11 show the chromatograms obtained for the degradation of triclopyr and mecoprop, respectively, and Fig. 12 reports the reaction rate constants for the removal of all three herbicides, of pyridine/aromatic ring and of TOC, using both photocatalysts.
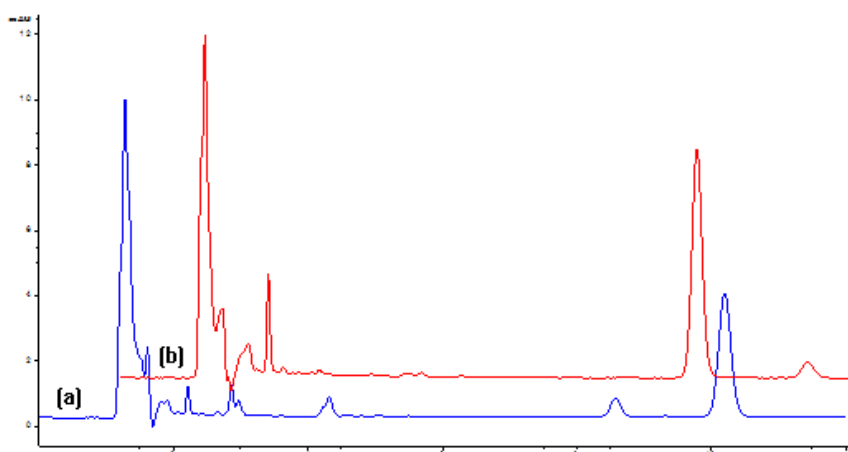
Fig. 10. Chromatograms obtained after 120 min of triclopyr degradation under UV irradiation, in the presence of TiO_2 Wackherr (a) and TiO_2 Degussa P25 (b). $\lambda_{det} = 230$ nm, RT(triclopyr) = 10.1 min.

A comparison of the chromatograms of Figs. 10 and 11 with those of Fig. 3 shows significant differences, which can also be observed in the case of the reaction rate constants. In the case of triclopyr removal, Degussa P25 was more efficient, whereas there was no difference in the kinetics of the pyridine ring degradation (Fig. 12). Higher removal efficiency by P25 was also observed in the case of mecoprop, together with a faster disappearance of the aromatic ring (Fig. 12).
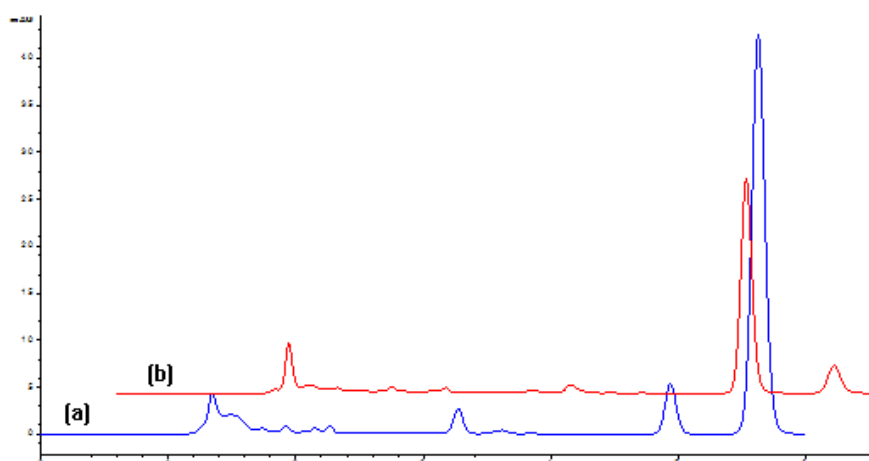

Fig. 11. Chromatograms obtained after 30 min of mecoprop degradation under UV irradiation, in the presence of TiO_2 Wackherr (a) and TiO_2 Degussa P25 (b). $\lambda_{det} = 228$ nm, RT(mecoprop) = 5.6 min.

It appears that the efficiency of photodegradation is influenced by both the substrate structure and the type of photocatalyst. Interestingly, TiO_2 Wackherr was more efficient than P25 in the degradation of picloram (this work), phenol and benzoic acid [17,23], while the reverse was true for triclopyr and mecoprop. Interestingly, the latter two compounds have lateral chains that would increase the hydrophobicity of the molecule, and all the cited substrates except phenol have carboxylic groups that would be at least partially deprotonated at pH 3 (which was adopted in the relevant irradiation experiments) [36]. The TiO_2 surface at pH 3 would be positively charged [37], which allows electrostatic interaction with the studied compounds.
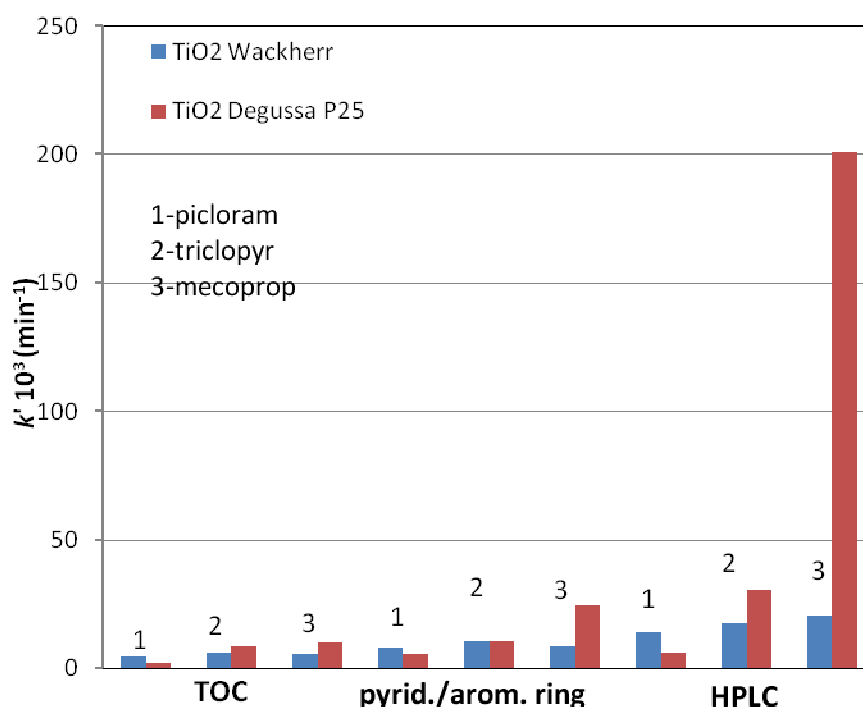

Fig. 12. Comparison of the reaction rate constants for photocatalytic degradation and mineralization of picloram, triclopyr and mecoprop, calculated for the period in which 80% of the starting component reacted.

The most hydrophobic substrates (triclopyr and mecoprop) could undergo a higher interaction with the TiO_2 surface, which is expected to favor the charge-transfer reactions at the expense of degradation by $^\bullet OH$ [38]. The effect of ethanol on picloram degradation (Figure 6) suggests that charge-transfer reactions would be more favored

on the surface of P25 compared with TiO_2 Wackherr. It might thus be reasonable to have higher activity of P25 toward the degradation of more hydrophobic substrates, which could undergo a higher interaction with the semiconductor surface.

4. Conclusions

A comparative study was made of the activity of TiO_2 Wackherr and Degussa P25 toward the photocatalytic degradation of picloram, a widely used herbicide. In contrast to visible light, UV irradiation yielded in both cases the degradation of picloram, but the transformation of the substrate was significantly faster in the presence of TiO_2 Wackherr. This was especially true at high photocatalyst loading and high substrate concentration, because TiO_2 Wackherr scatters UV radiation to a lesser extent than Degussa P25 (which helps preserving its photocatalytic efficiency at high loading) and is less affected by the decrease of degradation rate at high concentration of the substrate. These issues can largely compensate for the much lower surface area (8.5 *vs.* 50 m^2/g) of TiO_2 Wackherr compared to Degussa P25. Therefore, it is shown that a larger surface area does not necessarily yield higher photocatalytic activity, other factors being of comparable if not higher importance.

The photodegradation by TiO_2 Wackherr generated more UV-absorbing intermediates and at relatively higher concentration than Degussa P25. As a result, a complete mineralization was achieved in both cases after about 16 hours of irradiation. The inhibition of photocatalytic degradation observed in the presence of ethanol as a hydroxyl radical scavenger suggests that the process mainly involves $^{\bullet}OH$, especially in the case of TiO_2 Wackherr. Several degradation products that retain the pyridine ring were identified by LC–MS, GC–MS, and ^1H NMR. They are formed by elimination of the –COOH and –NH_2 groups and by replacement of a ring chlorine with –OH. There is also indirect evidence of the formation of unidentified aliphatic compounds bearing chlorine and nitrogen atoms. Results indicate that the efficiency of photocatalytic degradation is greatly influenced by the molecular structure of the substrate.

References

1 N.M. Soboleva, A.A. Nosovich, V.V. Goncharuk, J. Wat. Chem. Tech. 29 (2007) 72−89.

2 I.K. Konstantinou, D.G. Hela, T.A. Albanis, Environ. Pollut. 141 (2006) 555−570.

3 A. Matilainen, M. Sillanpää, Chemosphere 80 (2010) 351−365

4 D.R. Stapleton, I.K. Konstantinou, D. Mantzavinos, D. Hela, M. Papadaki, Appl. Catal. B: Environ. 95 (2010) 100−109.

5 W.H. Ahrens (Ed.), WSSA Herbicide Handbook, 7th ed., WSSA, Champaign, IL, 1994, pp. 235−237.

6 J.R. Bauer, R.D. Baker, R.W. Bovey, J.D. Smith, Weed Sci. 20 (1972) 305−309.

7 R.D. Wauchope, T.M. Buttler, A.G. Hornsby, P.W.M. Augustijn Beckers, J. P. Burt, Rev. Environ. Contam. Toxicol. 123 (1992) 1−157.

8 H. Kidd, D. R. James (Eds.), The Agrochemicals Handbook, Third ed., Royal Society of Chemistry Information Services, Cambridge, UK, 1991, pp. 10−12 (as updated).

9 D.B. Donald, A.J. Cessna, E. Sverko, N.E. Glozier, Environ. Health Perspect. 115 (2007) 1183−1191.

10 A. Ghauch, Chemosphere 43 (2001) 1109−1117.

11 M. Atiqur Rahman, M. Muneer, J. Environ. Sci. Health 40 (2005) 247−267.

12 A. Özcan, Y. Şahin, A.S. Koparal, M.A. Oturan, J. Hazard. Mater. 153 (2008) 718−727.

13 I. Pavlovic, C. Barriga, M.C. Hermosin, J. Cornejo, M.A. Ulibarri, Appl. Clay Sci. 30 (2005) 125−133.

14 L.P. Cardoso, J.B. Valim, J. Phys. Chem. Solids 67 (2006) 987−993.

15 J. Pignatello, Environ. Sci. Technol. 26 (1992) 944−951.

16 D.W. Hawker, J.L. Cumming, P.A. Neale, M.E. Bartkow B.I. Escher, Water Res. 45 (2011) 768−780.

17 D. Vione, C. Minero, V. Maurino, M.E. Carlotti, T. Picatonotto, E. Pelizzetti, Appl. Catal. B: Environ. 58 (2005) 79−88.

18 E.M. Abdel-Bary, E.A. Abdel-Razik, A.A. Sarhan, N.M. Abdel-Salam, Polym.-Plast. Technol. Eng. 35 (1996) 947−957.

19 D. Vione, V. Maurino, C. Minero, M. Vincenti, E. Pelizzetti, Chemosphere 44 (2001) 237−248.

20 S. Malato, P. Fernández-Ibáñez, M.I. Maldonado, J. Blanco, W. Gernjak, Catal. Today 147 (2009) 1−59.

21 C.S. Turchi, D.F. Ollis, J. Catal. 122 (1990) 178−185.

22 A. Mills, S. Morris, J. Photochem. Photobiol. A: Chem. 71 (1993) 75−83.

23 C. Minero, D. Vione, Appl. Catal. B: Environ. 67 (2006) 257−269.

24 S. Mozia, M. Tomaszewska, A.W. Morawski, Desalination 185 (2005) 449−456.

25 M.E. Carlotti, E. Ugazio, L. Gastaldi, S. Sapino, D. Vione, I. Fenoglio, B. Fubini, J. Photochem. Photobiol. B: Biol. 96 (2009) 130-135.

26 N. Daneshvar, D. Salari, A.R. Khataee, J. Photochem. Photobiol. A: Chem. 162 (2004) 317−322.

27 B.F. Abramović, V.B. Anderluh, A.S. Topalov, F.F. Gaál, Appl. Catal. B: Environ. 48 (2004) 213−221 (and references therein).

28 R.M Alberici, M.C. Canela, M.N. Eberlin, W.F. Jardim, Appl. Catal. B: Environ. 30 (2001) 389−397.

29 B.F. Abramović, V.B. Anderluh, A.S. Topalov, F.F. Gaál, J. Serb. Chem. Soc. 68 (2003) 961−970.

30 J.C. Colmenares, M.A. Aramendia, A. Marinas, J.M. Marinas, F.J. Urbano, J. Mol. Catal. A 331 (2010) 58−63.

31 A. Topalov, B. Abramović, D. Molnár-Gábor, J. Csanádi, O. Arcson, J. Photochem. Photobiol. A: Chem. 140 (2001) 249−253.

32 H.S. Son, S.J. Lee, I.H. Cho, K.D. Zoh, Chemosphere 57 (2004) 309−317.

33 D.V. Šojić, V.B. Anderluh, D.Z. Orčić, B.F. Abramović, J. Hazard. Mater. 168 (2009) 94−101.

34 X. Cai, J. Ye, G. Sheng, W. Liu, Environ. Sci. Pollut. Res. 4 (2009) 459−465.

35 S. Chiron, L. Comoretto, E. Rinaldi, V. Maurino, C. Minero, D. Vione, Chemosphere 74 (2009) 599−604.

36 A.E. Martell, R.M. Smith, R.J. Motekaitis, Critically selected stability constants of metal complexes database, version 4.0, 1997.

37 C. Minero, G. Mariella, V. Maurino, E. Pelizzetti, Langmuir 16 (2000) 2632-2641.

38 J.F. Montoya, J.A. Velasquez, P. Salvador, Appl. Catal. B: Environ. 88 (2009) 50-58.